

Dynamics of relativistic reconnection

Maxim Lyutikov ^{1,2,3}

Dmitri Uzdensky ⁴

¹ Physics Department, McGill University, 3600 rue University Montreal, QC, Canada H3A 2T8,

² Massachusetts Institute of Technology, 77 Massachusetts Avenue, Cambridge, MA 02139,
³ CITA National Fellow

⁴ Kavli Institute for Theoretical Physics, University of California, Santa Barbara, CA 93106

ABSTRACT

The dynamics of the steady-state Sweet–Parker-type reconnection is analyzed in relativistic regime when energy density in the inflowing region is dominated by magnetic field. The structure of reconnection layer (its thickness, inflow and outflow velocities) depends on the ratio of two large dimensionless parameters of the problem - magnetization parameter $\sigma \gg 1$ (the ratio of the magnetic to particle energy-densities in the inflowing region) and the Lundquist number S . The inflow velocity may be relativistic (for $S < \sigma$) or non-relativistic (for $S > \sigma$), while the outflowing plasma is moving always relativistically. For extremely magnetized plasmas with $\sigma \geq S^2$, the inflow four-velocity becomes of the order of the Alfvén four-velocity.

1. Introduction

Magnetic reconnection is widely recognized as a very important phenomenon in many laboratory and astrophysical plasmas (Biskamp 2000, Priest & Forbes 2000). It has been studied very extensively over the last 40 years, and a very significant progress has been made in understanding this process. However, historically, reconnection was of interest mostly to space physicists studying the Solar corona and the Earth’s magnetosphere and to researchers in magnetic confinement fusion. In all these environments, plasma flows are non-relativistic and the Alfvén velocity is usually much less than the speed of light (equivalently, magnetic energy density is much smaller than the particle rest mass energy density). Therefore it is not surprising that most of the progress on the subject has been made in non-relativistic regime.

Over the last decade however, it has been recognized that magnetic reconnection processes are also of great importance in high energy astrophysics, where dynamic behavior is often dominated by super-strong magnetic fields, with energy density $B^2/(8\pi)$ larger than the rest energy of the matter $\rho c^2 + \epsilon$. The best studied (but yet not completely understood) case is magnetized winds from pulsars. Models of pulsar magnetosphere (Goldreich & Julian 1969, Arons & Scharlemann 1979, Ruderman & Satherland 1975) predict that near the light cylinder most of the spin-down luminosity of a pulsar should be in a form of Poynting flux. Other possible examples of relativistic strongly magnetized media include jets emanating from magnetized accretion disks around Galactic black holes and neutron stars as well as Active Galactic Nuclei (e.g., Beskin 1997, Lovelace et al. 2002), magnetosphere of magnetars (Thompson & Duncan 1996, Thompson et al. 2002) and Gamma Ray Bursters (Lyutikov & Blandford 2002).

Dissipation of such super-strong magnetic fields may play an important role both for the global dynamics of the system and as a way to produce high energy emission. Magnetic reconnection has been proposed as the mechanism for acceleration of pulsar winds (Coroniti 1994, Kirk & Lyubarsky 2001) and GRB outflows (Spruit et al. 2001), and as a dissipation mechanism in AGN jets (Romanova & Lovelace 1992), Soft Gamma Ray Repeaters (Thompson & Duncan 1996), GRBs (Lyutikov & Blandford 2002, Spruit et al. 2001). In case of pulsar winds there are strong arguments that effective dissipation of magnetic field is, in fact, *needed* to account for the global dynamics of the Crab nebula (Kennel & Coroniti 1984; see also Michel 1994, Coroniti 1990, Melatos & Melrose 1996, Lyubarsky & Kirk 2001).

This provides the motivation for studying magnetic reconnection in strongly relativistic plasmas (to be defined below). Despite of the growing interest in relativistic magnetic reconnection, very little theoretical (let alone experimental!) work has been done on the subject so far. We are aware of only one analytical discussion of relativistic reconnection (Blackman & Field 1994) and two recent numerical works on particle dynamics in relativistic reconnection layers (Zenitani & Hoshino 2001, Larrabee et al. 2002).

In any theoretical analysis of magnetic reconnection, one first makes a number of approximations, e.g. incompressibility, two-dimensionality, the absence (or presence) of the axial magnetic field, etc. Then one formulates the set of MHD equations in a dimensionless form where the relative importance of various physical processes is represented by certain dimensionless parameters. After that one then tries to build a qualitative description of the reconnecting system by a small number of (also dimensionless) characteristic ratios. For example, in the simplest Sweet-Parker model of reconnection (e.g., Priest & Forbes 2000) one assumes incompressibility, uniform and constant resistivity η , and so on, and

one finds that the principal dimensionless parameter governing the system’s behavior is the Lundquist number $S \equiv V_A L / \eta \gg 1$, where V_A is the upstream Alfvén velocity and L is the size of the system. The other dimensionless plasma parameter, β - the ratio of thermal pressure to magnetic field energy density, turns out not to be as important, at least in the first approximation. Correspondingly S^{-1} plays a role of the small parameter on which all further asymptotic expansions and boundary layer analysis are based. One then seeks to find out how the dimensionless characteristics of the system, such as the reconnection layer’s aspect ratio δ/L and the ratio of the incoming velocity to the Alfvén velocity scale with S as $S \rightarrow \infty$.

The generalization of reconnection to the relativistic case requires an introduction of one more (in addition to S) principal dimensionless parameter that should describe how far in relativistic regime we are. This parameter is σ , the ratio of the magnetic field energy density to the plasma’s rest mass energy density in the inflow region. We are now in position to define what we mean by relativistic reconnection: we consider a case when magnetic energy density in the flowing plasma dominates over particle energy density, $\sigma \gg 1$. During reconnection magnetic energy is dissipated and transformed into plasma thermal energy and later into bulk motion. Since $\sigma \gg 1$, energy per baryon becomes much larger than $m_p c^2$ and so we get relativistically hot plasma in the reconnection layer. Expansion of plasma along the reconnection layer will produce relativistic bulk motions downstream. In relativistic regime, $\sigma \gg 1$, the Alfvén velocity becomes relativistic, $V_A = \sqrt{\sigma/(1+\sigma)}c \simeq c$, so that under certain conditions (to be determined later) the upstream flow is expected to be relativistic as well.

Thus, in case of relativistic reconnection there are two very large dimensionless parameters, S and σ . As we shall see below, one gets two different regimes depending on the ratio of these parameters: in one regime the incoming (the upstream) flow is ultra-relativistic, while in the other it is non-relativistic.

In this paper we present a relativistic generalization of the simplest model of magnetic reconnection — the Sweet–Parker model — to strongly relativistic plasmas. This is a simple two-dimensional resistive MHD model, presented in Figure 1. We assume that the reconnection layer has a rectangular shape with a width L and thickness $\delta \ll L$. The width L of the reconnection layer is determined by the global system size and thus, for the purposes of studying magnetic reconnection, is a fixed prescribed quantity. Also prescribed are the magnetic field strength and the baryon density and pressure in the ideal-MHD inflow region above and below the reconnection layer. In contrast, the thickness δ of the reconnection region, as well as some other parameters such as the plasma inflow and outflow velocity, are not prescribed and need to be calculated as a part of the analysis.

We basically follow the steps of the Sweet–Parker analysis while taking into account relativistic effects, such as relativistic contraction and inertia of magnetic field. As the plasma enters the reconnection layer it slows down coming to a halt at stagnation point. At the same time the magnetic energy is dissipated and converted into internal energy of pair-rich plasma. In the out-flowing region the plasma is accelerated by the pressure gradient in x direction reaching some terminal relativistic velocity γ_{out} . We assume that energy losses are not important and the total energy of a fluid element (or at least a large fraction) stays within this fluid element, providing the corresponding amount of pressure support. Though generally radiative losses may be important, we expect that the reconnecting plasma will be optically thick to Thomson scattering after it's temperature becomes weakly relativistic, $T \geq 20$ keV. Above this temperature an efficient pair production process will start (e.g., Goodman 1986) inside the reconnection current layer trapping the radiation. The role of pair production in increasing the optical depth is an interesting question in itself and deserves further study (Thompson 1994). It lies, however, outside the scope of our paper; here we simply assume that the plasma is optically thick inside the reconnection layer and so the released magnetic field energy cannot leave the system and is therefore available for accelerating plasma downstream.

2. Relativistic reconnection formulation

The basic equations include the relativistic Ohm's law and the relativistic dynamics, Maxwell's and mass conservation equations (Lichnerowicz 1967):

$$T_{,i}^{ij} = 0, \tag{1}$$

$$F_{,i}^{*ij} = 0, \tag{2}$$

$$(\rho u^i)_{,i} = 0 \tag{3}$$

where

$$T^{ij} = (w + b^2 + \epsilon^2)u^i u^j + (p + \frac{b^2 + \epsilon^2}{2})g^{ij} - b^i b^j - \epsilon^i \epsilon^j \tag{4}$$

is the stress-energy tensor, w is the plasma proper enthalpy, ρ is proper plasma density and p is pressure, $b^2 = b_i b^i$ and $\epsilon^2 = \epsilon^i \epsilon_i$ are the plasma proper magnetic and electric energy density times 4π , p is pressure, $u^i = (\gamma, \gamma\beta)$ are the plasma four-velocity, Lorentz-factor and three-velocity, g^{ij} is the metric tensor, $b_i = \frac{1}{2}\eta_{ijkl}u^j F^{kl}$ are the four-vector of magnetic field, Levy-Chevita tensor and electro-magnetic field tensor and $\epsilon_i = u^j F_{ji}$ is the four-vector of the electric field.

The choice of the stress-energy tensor deserves some discussion. The stress-energy tensor (4) is a full electro-magnetic field plus matter tensor; this is *not* the relativistic

magneto-hydrodynamic (RMHD) stress-energy tensor. The reason is that in the frame work of RMHD it is assumed that one of the electro-magnetic invariants is not equal to 0 and electro-magnetic stress energy tensor can be diagonalized. Equivalently, this implies that there is a reference frame where electric field is equal to 0. In case of resistive RMHD such frame may not exist, since, generally, there are resistive electric fields in the plasma rest-frame either along the null magnetic line (this violates then the $B^2 - E^2 > 0$ condition of the ideal MHD), or field aligned electric fields (this violates $\mathbf{E} \cdot \mathbf{B} = 0$ condition). In the full relativistic approach the resistive electric field contributes to plasma energy density, energy fluxes and stresses. Nevertheless, we can still define the plasma rest frame by requiring that in that frame the electric fields ϵ are only of resistive nature. We then obtain the stress-energy tensor (4).

In what follows we will be using both the rest frame quantities (\mathbf{b} , ϵ , p , w , ρ_e^* , ρ^* for renormalized magnetic and electric fields, pressure enthalpy and charge and mass densities as well as laboratory quantities \mathbf{B} , \mathbf{E} , ρ_e , ρ (pressure and enthalpy are defined only in the rest frame).

2.1. Relativistic Ohm's law

Relativistic Ohm's law is

$$j^j = (ju)u^j + \frac{1}{\eta} F^{ik} u_k \quad (5)$$

where η is the plasma resistivity (e.g. Lichnerowicz 1967). In 3-D notations (Greek indexes =1,2,3) this gives

$$\begin{aligned} j^0 &\equiv \rho_e = \frac{(\mathbf{j} \cdot \boldsymbol{\beta})}{\beta^2} - \frac{1}{\eta\gamma} (\mathbf{E} \cdot \boldsymbol{\beta}) \\ \mathbf{j} &= (j^0 - (\mathbf{j} \cdot \boldsymbol{\beta})) \gamma^2 \boldsymbol{\beta} + \frac{\gamma}{\eta} (\mathbf{E} + (\boldsymbol{\beta} \times \mathbf{B})) \end{aligned} \quad (6)$$

which can be written

$$\left(\delta^{\alpha\beta} - \frac{\beta^\alpha \beta^\beta}{\beta^2} \right) \left(j_\beta - \frac{\gamma}{\eta} E_\beta \right) = \frac{\gamma}{\eta} (\boldsymbol{\beta} \times \mathbf{B})|^\alpha \quad (7)$$

The form (7) of the relativistic Ohm's law shows that for $(\mathbf{j} \cdot \boldsymbol{\beta}) = 0$ and $(\mathbf{E} \cdot \boldsymbol{\beta}) = 0$ the relativistic effects change the conductivity

$$\eta \rightarrow \frac{\eta}{\gamma} \quad (8)$$

This can be understood if one notices that in the plasma rest frame the electric field $\epsilon = E/\gamma$, and, since for $(\mathbf{j} \cdot \beta) = 0$ the current in the rest frame is \mathbf{j}

$$\mathbf{j} = \frac{\epsilon}{\eta} \quad (9)$$

2.2. Main equations

For stationary flow the energy and momentum flux conservation can be rewritten

$$\begin{aligned} \nabla_\alpha (\gamma^2 (w + b^2) \beta) &= 0 \\ \nabla_\beta (\gamma^2 w \beta^\alpha \beta^\beta - p \delta^{\alpha\beta}) &= F^{\alpha\beta} j_\beta = \rho_e E^\alpha + (\mathbf{j} \times \mathbf{B})^\alpha \end{aligned} \quad (10)$$

The Maxwell's equations then become

$$\begin{aligned} \mathbf{j} &= \frac{1}{4\pi} \nabla \times \mathbf{B} \\ (\nabla \times \mathbf{E}) &= 0 \\ \text{div} \mathbf{E} &= 4\pi \rho_e \end{aligned} \quad (11)$$

The equation of continuity is

$$\text{div} \gamma \beta \rho^* = 0 \quad (12)$$

The above equations plus the equation of state form a system of 15 equations for 15 variables $\beta, \mathbf{E}, \mathbf{B}, \mathbf{j}, \rho_e, \rho, p$.

Following the Sweet–Parker model we neglect possible field-aligned electric fields and currents. Then the only non-vanishing components of electric field and current are E_z and j_z . Since the velocity lies in the $x - y$ plane from eq. (6) it follows that the charge density $\rho_e \equiv j^0 = 0$. This is an important simplification since generally for relativistic plasma the charge density can not be neglected.

2.3. Magnetization parameter

We assume that far in the incoming region plasma is cold and strongly magnetically dominated. In the incoming region, well outside the reconnection layer, the restive electric field is vanishing and can be neglected. We introduce a frame-invariant ratio of the rest energy density of magnetic field and particles

$$\sigma = \frac{b_{\text{in}}^2}{\rho^*} \gg 1 \quad (13)$$

This definition of σ is equivalent to the ratio of Poynting to particle fluxes in the incoming region (c.f., Kennel & Coroniti 1984). For example, for pulsar winds initially (near the light cylinder) $\sigma \sim 10^3 - 10^6$ (e.g., Arons & Scharlemann 1979).

We have defined the σ -parameter in a frame-invariant way in terms of the rest-frame quantities. Alternative definition involves the laboratory frame fields and densities

$$\sigma_l = \frac{B_{\text{in}}^2}{\rho} = \gamma_{\text{in}}\sigma \quad (14)$$

It is straightforward to express the results in terms of σ_l instead of σ .

3. Flow along the velocity separatrix

In non-relativistic reconnection an important model problem is the flow of plasma along the velocity separatrix $x = 0$ (e.g., Priest & Forbes 2000). In this case a simple equation relating magnetic field strength and inflow velocity can be obtained using only Ohm's law (7). Solving this equation for a given velocity (or vice versa for a given magnetic field) profile would allow us to find an example of velocity and magnetic distributions.

The relativistic Ohm's law (7) along the velocity separatrix can be written as

$$j(y) \equiv j_z(x = 0, y) = \frac{\gamma(y)}{\eta} (E_z - \beta_y B_x). \quad (15)$$

For a more compact notation we introduce $B(y) \equiv B_x(x = 0, y) > 0$ and also $\beta(y) \equiv -\beta_y(x = 0, y) > 0$ (here we changed the sign so that β is positive for convenience). Then, the above equation for Ohm's law can be rewritten as

$$j(y) \equiv j_z(x = 0, y) = \frac{\gamma(y)}{\eta} [E_z + \beta(y)B(y)]. \quad (16)$$

In a steady case Maxwell's equation gives $\nabla \times E = 0$, and hence, using $\partial/\partial z = 0$,

$$E_z(x, y) = \text{const} \equiv E. \quad (17)$$

In the ideal region above the layer, Ohm's law gives

$$E = -\beta_{\text{in}} B_{\text{in}}, \quad (18)$$

where $B_{\text{in}} \equiv B(y \gg \delta)$, and $\beta_{\text{in}} \equiv \beta(y \gg \delta)$.

Using the first of the Maxwell equations (11) in laboratory frame, we find

$$\eta \frac{\partial B}{\partial y} = -\gamma(E + \beta B), \quad (19)$$

or, using our expression for E ,

$$\frac{\eta}{\gamma} \partial_y \hat{B} = \beta_{\text{in}} - \beta \hat{B}, \quad (20)$$

where $\hat{B} \equiv B/B_{\text{in}}$. This equation should be supplemented by the boundary conditions $\hat{B}(y = 0) = 0$, $\beta(y = 0) = 0$ and $\hat{B}(y \rightarrow \pm\infty) = \pm 1$, $\beta(y \rightarrow \pm\infty) = \pm\beta_{\text{in}}$. Equation (20) relates the two functions — inflow velocity and magnetic field along the separatrix. For example, for a given $\beta(y)$ the two boundary conditions for the first-order ODE (20) determine the solution $\hat{B}(y)$ and put a constraint on the parameters η , β_{in} , and δ .

For example, eq. (20) can be resolved for $\hat{B}(y)$ for a given $\beta(y)$:

$$\hat{B}(y) \equiv \frac{B(y)}{B_{\text{in}}} = \frac{\beta_{\text{in}}}{\eta} e^{-\frac{\int^y \beta(y') \gamma(y') dy'}{\eta}} \int^y e^{\frac{\int^{y'} \beta(y'') \gamma(y'') dy''}{\eta}} \gamma(y') dy'. \quad (21)$$

The boundary condition $\hat{B}(y = 0) = 0$ is automatically satisfied, while the condition $\hat{B}(y = \delta) = 1$ serves as an eigenvalue problem for $\delta(\eta, \beta_{\text{in}})$.

As an example, consider a case where the inflow four-velocity, $u \equiv \gamma\beta$, is a linear function of distance along the y axis:

$$u = \begin{cases} u_{\text{in}} \frac{y}{\delta} & \text{if } |y| < \delta \\ u_{\text{in}} & \text{if } |y| > \delta \end{cases} \quad (22)$$

By definition, δ is the scale on which the inflow velocity changes from initial $u = u_{\text{in}}$ to zero.

Introducing dimensionless parameter $Y \equiv \delta/\eta$ ($Y = c\delta/\eta$ in dimensional units) and rescaling coordinate y by δ , $\tilde{y} = y/\delta$, the magnetic field is then determined by

$$\frac{B(\tilde{y} \leq 1)}{B_{\text{in}}} = \frac{u_{\text{in}} Y}{\sqrt{1 + u_{\text{in}}^2}} e^{-u_{\text{in}} \tilde{y}^2 Y/2} \int_0^{\tilde{y}} e^{u_{\text{in}} \tilde{y}'^2 Y/2} \sqrt{1 + \tilde{y}'^2 u_{\text{in}}^2} d\tilde{y}' \quad (23)$$

Parameter Y here is an implicit function of u_{in} given by the condition $B(1) = B_{\text{in}}$. Numerical solution $Y(u_{\text{in}})$ is plotted in Figure 2. The corresponding magnetic field profiles for different values of u_{in} are plotted in Figure 3.

Several important conclusions can be drawn from this exercise: (i) both the four velocity and magnetic field have *the same* typical scale $\sim \delta$; (ii) both in the non-relativistic ($u_{\text{in}} \ll 1$) and strongly relativistic ($u_{\text{in}} \gg 1$) regimes the ratio $Y = c\delta/\eta$ asymptotically

becomes inversely proportional to the four-velocity of the incoming flow, $Y \sim 1/u_{\text{in}}$, in agreement with the Sweet–Parker theory (in the non-relativistic case). Asymptotic scalings of $Y(u_{\text{in}})$ for $u_{\text{in}} \ll 1$ and $u_{\text{in}} \gg 1$ are analyzed in Appendix A. (iii) in the case of strongly relativistic inflow, there is a thin sub-layer near the neutral point, $y = 0$, with the thickness $\delta_{\text{nr}} \sim \delta/u_{\text{in}}$, where the flow becomes non-relativistic.¹ Outside of this sub-layer, the function $\hat{B}(\tilde{y})$ approaches a universal shape in the limit $u_{\text{in}} \rightarrow \infty$. Inside the sub-layer the magnetic field becomes linear,

$$B \sim \frac{y}{\eta} B_{\text{in}}, \text{ for } y \ll \delta/u_{\text{in}} \quad (24)$$

Typical magnetic field in the non-relativistic sub-layer is

$$B_{\text{nr}} \sim \frac{\delta}{\eta u_{\text{in}}} B_{\text{in}} \sim \frac{B_{\text{in}}}{u_{\text{in}}^2} \ll B_{\text{in}} \quad (25)$$

while the typical current density is

$$j_{\text{nr}} \sim \frac{B_{\text{in}}}{\eta} \sim \frac{B_{\text{in}}}{\gamma_{\text{in}} \delta} \quad (26)$$

Here lies a qualitative difference between the non-relativistic and relativistic reconnection layer. In the non-relativistic Sweet–Parker theory the thickness of the layer is defined by the magnitude of current density at the center $y = 0$. In the case of relativistic inflow ($\gamma_{\text{in}} \gg 1$), the current flowing in the bulk of the flow $j \sim B_{\text{in}}/\delta$ is much stronger than typical current on the midplane.

The example in this section is an illustration only, invoked in order to demonstrate a possible relation between δ and β_{in} . We use here only Ohm’s law to establish such a connection; in reality, the velocity profile needs to be determined self-consistently by solving the entire 2D problem, including the equation of motion.

4. Relativistic Sweet-Parker model

In this section we use Ohm’s law and the conservation laws for energy and particle flux and do not solve the momentum equation. All the estimates below are made up to the order of magnitude, or, more precisely, how they scale with two parameters, S and σ .

¹Because of the very large proportionality coefficient between Y and u_{in} in the strongly-relativistic case, this sub-layer develops only for very large (of order 10^2 and greater) values of u_{in} , as can be seen from Figure 3.

Estimating the current in the reconnection layer

$$j_z \sim \frac{B}{\delta} \sim \frac{\gamma_{\text{in}} \beta_{\text{in}} B_{\text{in}}}{\eta} \quad (27)$$

we find

$$\beta_{\text{in}} \gamma_{\text{in}} \sim \frac{\eta}{\delta c} \quad (28)$$

(we have restored the velocity of light here to make the right-hand side explicitly dimensionless). Introducing relativistic Lundquist number

$$S = \frac{Lc}{\eta} \gg 1 \quad (29)$$

eq. (28) can be rewritten

$$\beta_{\text{in}} \gamma_{\text{in}} \sim \frac{L}{\delta} \frac{1}{S} \quad (30)$$

This is the first basic equation of the model.

The energy flux and the particle conservation give

$$\begin{aligned} \gamma_{\text{in}}^2 \beta_{\text{in}} (1 + \sigma) \rho_{\text{in}}^* L &= \gamma_{\text{out}}^2 \beta_{\text{out}} \rho_{\text{out}}^* \delta \\ \gamma_{\text{in}} \rho_{\text{in}}^* \beta_{\text{in}} L &= \gamma_{\text{out}} \rho_{\text{out}}^* \beta_{\text{out}} \delta \end{aligned} \quad (31)$$

In writing down these equations we have assumed that magnetic energy is fully spent on acceleration of baryons in the downstream flow. This assumes that all the electron-positron pairs created in the reconnection layer have annihilated.

Then it follows that

$$\gamma_{\text{in}} (1 + \sigma) = \gamma_{\text{out}} \quad (32)$$

and

$$\begin{aligned} \frac{\delta}{L} &\sim \frac{1}{S \beta_{\text{in}} \gamma_{\text{in}}} \\ \frac{\rho_{\text{in}}^* \beta_{\text{in}}}{\rho_{\text{out}}^* \beta_{\text{out}}} &= (1 + \sigma) \frac{\delta}{L} \end{aligned} \quad (33)$$

Equation (32) relates the velocity in the outflowing region to the inflow velocity and magnetization parameter. For small $\sigma \ll 1$ eq. (32) reproduces the familiar non-relativistic result that the outflowing velocity is of the order of the inflowing Alfvén speed: $\beta_{\text{out}} \sim \sqrt{2\sigma} = B/c\sqrt{4\pi\rho} = V_A/c$. In the relativistic regime, $\sigma \gg 1$, the outflowing velocity is always relativistic so that $\beta_{\text{out}} \sim 1$. It is remarkable, that in relativistic reconnection the

Lorentz factor of the outflowing plasma is *much larger* than the Lorentz factor of Alfvén waves in the inflowing region γ_A : $\gamma_{\text{out}} \sim \sigma \gamma_{\text{in}} = \gamma_A^2 \gamma_{\text{in}}$, where $\gamma_A \sim \sqrt{\sigma}$.

Eqns. (32) and (33) are general relations for four unknown quantities: δ , γ_{in} , γ_{out} and $\rho_{\text{in}}^*/\rho_{\text{out}}^*$. In order to resolve this system we need to use the momentum equations and find the structure of the flow inside the reconnection region, but this is a difficult task. An alternative way to proceed is to assume incompressibility of the plasma in its rest-frame $\rho_{\text{in}}^* = \rho_{\text{out}}^*$ (c.f., Blackman & Field 1994). Incompressibility may be due to, for example, a significant longitudinal field component B_z . It is expected that the assumption of incompressibility will be justified as long as the inflowing plasma velocity is smaller than the fast magneto-sonic velocity, which in our case is similar to the Alfvén velocity.

Below we show that for a given value of S the inflowing velocity increases with the magnetization parameter σ reaching at $\sigma \sim S^2$ the Alfvén velocity. For such strong magnetization the compressibility of plasma will become important. For any $\sigma \ll S^2$ the incompressibility is expected to be a good approximation.

The assumption of incompressibility gives in relativistic limit $\sigma \gg 1$

$$\beta_{\text{in}} \gamma_{\text{in}} L = \gamma_{\text{out}} \delta \quad (34)$$

and

$$\beta_{\text{in}} = \sigma \frac{\delta}{L} \quad (35)$$

(here we dropped β_{out} because we expect an ultra-relativistic outflow with $\beta_{\text{out}} \approx 1$.)

Eq. (35) and the approximate Ohm’s law (30) form a system of two equations for the thickness of the reconnection layer δ and the inflow velocity β_{in} . There are two generic regimes (limiting cases) of relativistic reconnection: (i) relativistic inflow $\gamma_{\text{in}} \gg 1$ and (ii) non-relativistic inflow $\beta_{\text{in}} \ll 1$.

4.1. Non-relativistic inflow $\beta_{\text{in}} \ll 1$

Using eqns. (35) and (30) we find

$$\beta_{\text{in}} \sim \frac{L}{\delta} \frac{1}{S} \sim \frac{\sigma \delta}{L} \quad (36)$$

Thus,

$$\frac{\delta}{L} \sim \frac{1}{\sqrt{S\sigma}} \sim \frac{\beta_{\text{in}}}{\sigma} \sim \frac{1}{S\beta_{\text{in}}} \quad (37)$$

and finally

$$\beta_{\text{in}} \sim \sqrt{\frac{\sigma}{S}} \sim \sqrt{\frac{2}{S}} \gamma_A \quad (38)$$

where $\gamma_A = \sqrt{2\sigma}$ is the Lorentz factor of the Alfvén wave velocity in the incoming region. Since by assumption $\beta_{\text{in}} \ll 1$ the non-relativistic inflow velocity is realized for $\sigma \ll S$.

Thus, for a given σ the inflow velocity is inversely proportional to the square root of the Lundquist number, similar to the classical non-relativistic Sweet-Parker model.

4.2. Relativistic sub-alfvenic inflow $1 \ll \gamma_{\text{in}} \ll \sqrt{2\sigma}$

When $\beta_{\text{in}} \approx 1$ from eq. (35) it follows

$$\frac{\delta}{L} \sim \frac{1}{\sigma} \quad (39)$$

and

$$\begin{aligned} \gamma_{\text{out}} &\sim \frac{\sigma^2}{S} \\ \gamma_{\text{in}} &\sim \frac{\sigma}{S} \end{aligned} \quad (40)$$

For consistency we need $\sigma \gg S$ (since we have always assumed relativistic motion $\gamma \gg 1$).

The ratio of the inflowing plasma Lorentz factor to the Alfvén wave Lorentz factor is

$$\frac{\gamma_{\text{in}}}{\gamma_A} \sim \frac{\sqrt{\sigma/2}}{S} \quad (41)$$

Since the inflowing plasma should be sub-alfvenic for the incompressibility assumption to hold, it is required that

$$\sigma \ll 2S^2 \quad (42)$$

Thus the incompressible relativistic inflow case is applicable for

$$S \ll \sigma \ll 2S^2 \quad (43)$$

4.3. Relativistic alfvenic inflow $\gamma_{\text{in}} \sim \sqrt{2\sigma}$

If $\sigma \geq 2S^2$ the required inflow velocity becomes of the order of the Alfvén velocity and the assumption of incompressibility should break down. Since the inflow velocity

cannot exceed the Alfvén velocity for causal reasons, we assume that $\gamma_{\text{in}} \sim \gamma_A = \sqrt{2\sigma}$. The parameters of the reconnection layer then become

$$\begin{aligned} \gamma_{\text{out}} &\sim \sqrt{2}\sigma^{3/2} \\ \delta &\sim \frac{1}{\sqrt{2\sigma S}} \\ \frac{\rho_{\text{in}}^*}{\rho_{\text{out}}^*} &\sim \sqrt{\frac{\sigma}{2}} \frac{1}{S} \geq 1 \end{aligned} \quad (44)$$

5. Bohm diffusion

In the preceding section we have derived how the flow variables (first of all the inflow velocity) scale with two parameters of the model, S and σ . For astrophysical applications it is often useful to have a qualitative estimate of the maximum possible reconnection rate in a given system. The maximum reconnection rate corresponds to the maximum value for resistivity and thus the minimal Lundquist number. This resistivity may be estimated using Bohm’s arguments that the maximum diffusion coefficient in magnetized plasmas cannot be much larger than $r_L v$, where r_L is the Larmor radius and v is the typical velocity of electrons (of the order of the speed of light in our case). Thus,

$$\eta \sim \frac{c^2}{\omega_B} \quad (45)$$

and we find

$$S \sim \frac{L}{r_L} \quad (46)$$

$$\delta \sim \frac{r_L}{\beta_{\text{in}} \gamma_{\text{in}}} \quad (47)$$

$$\beta_{\text{in}}^2 \gamma_{\text{in}} \sim \sigma \frac{r_L}{L} \quad (48)$$

Note, that in this case, as β_{in} approaches the velocity of light the reconnection layer becomes microscopically thin. One may expect that the fluid picture will become inapplicable at this point.

For non-relativistic inflow velocity the assumption of Bohm diffusion gives

$$\begin{aligned} \delta &\sim \sqrt{\frac{r_L L}{\sigma}} \\ \beta_{\text{in}} &\sim \sqrt{\frac{\sigma r_L}{L}} \end{aligned} \quad (49)$$

while for relativistic inflow velocity

$$\begin{aligned} \delta &\sim \frac{r_L}{\gamma_{\text{in}}} \\ \gamma_{\text{in}} &\sim \sigma \frac{r_L}{L} \end{aligned} \tag{50}$$

which requires $\sigma r_L/L > 1$. In the case of relativistic inflow velocity and under the assumption of Bohm diffusion the thickness of the reconnection layer becomes smaller than the external gyro-radius.

Equations (48) and the two limiting cases (49) and (50) give a useful "order-of-magnitude" estimates of the potential efficiency of reconnection in relativistic plasma.

6. Discussion

We have considered the dynamics of the relativistic Sweet-Parker reconnection under the assumption that the inflow region's energy density is dominated by magnetic field. We have found three generic regimes depending on the ratio of the magnetization parameter σ to the Lundquist number S : (i) non-relativistic inflow velocity, $\sigma \ll S$; (ii) relativistic sub-alfvenic inflow velocity, $S \ll \sigma \ll 2S^2$; (iii) relativistic alfvenic inflow velocity, $\sigma \geq 2S^2$. For the first two regimes plasma flow may be assumed incompressible, while for the alfvenic inflow velocity compressibility is important.

An apparent drawback of our approach is that we did not solve in a self-consistent way both the momentum and energy equations. This is a common flaw of many models of reconnection based on the Sweet-Parker approach. One can say that the role of the energy equation is to determine how compressible the plasma is. Conventionally, the simplest Sweet-Parker model does not include the energy balance equation with all its subtleties arising from possible radiation and conducting cooling effects; instead, it just replaces the energy balance equation with the incompressibility condition. In the absence of strong cooling or when a strong axial magnetic field component is present, the compressibility effects are indeed not important, at least in a rough, order-of-magnitude analysis. One then combines the incompressibility condition with the momentum equation and Ohm's law to arrive at the Sweet-Parker reconnection scaling. In our analysis we also assume incompressibility but then we use the energy conservation instead of the momentum equation; in the absence of energy losses these two approaches are, of course, equivalent and lead to the same results.

In spite of the incompressibility assumption our approach represents a step forward in understanding relativistic reconnection as compared to the view of Blackman & Field

(1994). Using the same incompressibility assumption they were able to determine only the ratio of inflow and outflow velocities, while we find both these quantities separately, expressed in terms of external magnetization and the Lundquist number. We have also found a possible structure of the relativistic reconnection layer.

For astrophysical applications, we were able to provide order-of-magnitude estimates of reconnection rates in relativistic plasma (eq. 48), which should be used instead of the often *ad hoc* assumptions of reconnection rates in strongly magnetized plasmas of pulsar winds and AGN jets. An important result is that under certain conditions the inflow velocity may become relativistic insuring very efficient dissipation of magnetic energy.

We would like to thank Eric Priest, Vladimir Pariev, Eric Blackman, Chris Thompson and Alissa Nedossekina for comments on the manuscript. This research was supported by the NSF grant NSF-PHY99-07949. DU would like to thank CITA for hospitality during his visit.

REFERENCES

- Arons, J., Scharlemann, E. T., 1979, ApJ, 231, 854
- Beskin, V. S., 1997, Uspekhi Fizicheskikh Nauk, 40, 659
- Biskamp, D., 2000, “Magnetic reconnection in plasmas”, Cambridge University Press
- Blackman, E. G., Field, G. B., 1994, Physical Review Letters, 72, 494
- Coroniti, F. V., 1990, ApJ, 349, 538
- Goldreich, P., Julian, W. H., 1969, ApJ, 157, 869
- Goodman, J., 1986, ApJ, 308, 47
- Kennel, C. F., & Coroniti, F. V. 1984a, ApJ, 283, 694 ; 1984b, ApJ, 283, 710
- Larrabee, D.A., Lovelace R.V.E., Romanova M.M., astro-ph/0210045
- Lichnerowicz, A., 1967, ”Relativistic Magnetohydrodynamics”, Benjamin, New York
- Lovelace, R. V. E., Li, H., Koldoba, A. V., Ustyugova, G. V., Romanova, M. M., 2002, ApJ, 572, 445
- Lyubarsky, Y., Kirk, J. G., 2001, ApJ, 547, 437

- Lyutikov, M., Blandford. R., 2002, in preparation
- Melatos, A., Melrose, D. B., 1996, MNRAS, 279, 1168
- Michel, F. C., 1994 ApJ, 431, 397
- Priest, E., Forbes, T., 2000, “Magnetic reconnection : MHD theory, applications”,
Cambridge University Press
- Romanova, M. M., Lovelace, R. V. E., 1992, A&A, 262, 26
- Ruderman, M. A., Sutherland, P. G., 1975, ApJ, 196, 51
- Sheffield, J., 1994, Reviews of Modern Physics, 66, 1015
- Spruit, H. C., Daigne, F., Drenkhahn, G., 2001, A&A, 369, 694
- Thompson, C., 1994, MNRAS, 270, 480
- Thompson, C., Duncan, R. C., 1996, ApJ, 473, 322
- Thompson, C., Lyutikov, M., Kulkarni, S. R., 2002, ApJ, 574, 332
- Zenitani, S., Hoshino, M., 2001, ApJ, 562, 63

A. Asymptotic scaling of $Y(u_{\text{in}})$

In this appendix we investigate the asymptotic behavior of the function $Y(u_{\text{in}})$ in the case of the 4-velocity field $u(y)$ described by equation (22), for two limiting regimes, $u_{\text{in}} \rightarrow 0$ and $u_{\text{in}} \rightarrow \infty$.

We start by rewriting equation (22) in terms of rescaled coordinate $\tilde{y} = y/\delta$:

$$\frac{\partial \hat{B}(\tilde{y})}{\partial \tilde{y}} = Y \gamma (\beta_{\text{in}} - \beta B). \quad (\text{A1})$$

Now let us integrate this equation from 0 to 1 and use the boundary conditions $\hat{B}(0) = 0$ and $\hat{B}(1) = 1$. We get

$$B(1) - B(0) = 1 = Y \beta_{\text{in}} \int_0^1 \gamma(\tilde{y}) d\tilde{y} - Y \int_0^1 u(\tilde{y}) B(\tilde{y}) d\tilde{y}. \quad (\text{A2})$$

For the velocity field given by equation (22), i.e. $u(\tilde{y}) = u_{\text{in}}\tilde{y}$, we then have

$$Y^{-1} = \beta_{\text{in}} \int_0^1 \gamma(\tilde{y}) d\tilde{y} - u_{\text{in}} \int_0^1 \tilde{y} B(\tilde{y}) d\tilde{y}. \quad (\text{A3})$$

Using the relationship $\gamma = \sqrt{1 + u^2}$, the integral in the first term on the right-hand side can be computed exactly, with the result

$$\int_0^1 \gamma(\tilde{y}) d\tilde{y} = \frac{1}{u_{\text{in}}} \int_0^{u_{\text{in}}} \sqrt{1 + u^2} du = \frac{\sqrt{1 + u_{\text{in}}^2}}{2} + \frac{1}{2} \ln(u_{\text{in}} + \sqrt{1 + u_{\text{in}}^2}). \quad (\text{A4})$$

In the strongly relativistic limit $u_{\text{in}} \rightarrow \infty$ this expression can be expanded as

$$\int_0^1 \gamma(\tilde{y}) d\tilde{y} = \frac{u_{\text{in}}}{2} + \frac{1}{2} \ln u_{\text{in}} + O(1). \quad (\text{A5})$$

As for the second term, we note that in the strongly relativistic limit there is a thin non-relativistic boundary sub-layer of thickness $\delta_{nr} \sim \delta/u_{\text{in}}$; inside this sub-layer $\hat{B}(y)$ behaves linearly, with the slope that, as we shall see later, is inversely proportional to u_{in} . However, what is important for us here, outside of this infinitesimally thin sub-layer the function $\hat{B}(\tilde{y})$ approaches a certain universal shape, $\hat{B}_{\text{rel}}(\tilde{y})$ in the limit $u_{\text{in}} \rightarrow \infty$. This conclusion follows from our numerical solutions presented in Figure 3. Ignoring the non-relativistic sublayer's contribution to the integral in the second term on the right-hand side of equation (A3), we can then estimate this integral as

$$\int_0^1 \tilde{y} \hat{B}(\tilde{y}) d\tilde{y} \rightarrow \int_0^1 \tilde{y} \hat{B}_{\text{rel}}(\tilde{y}) d\tilde{y}, \quad \text{as } u_{\text{in}} \rightarrow \infty, \quad (\text{A6})$$

Combining this result with the result (A5) derived for the first term on the right-hand side of equation (A3), we finally can write the following expression:

$$Y = \frac{1}{A_{\text{rel}} u_{\text{in}} + \frac{1}{2} \ln u_{\text{in}} + C}, \quad (\text{A7})$$

where we used the identity $\int_0^1 \tilde{y} d\tilde{y} = 1/2$ and defined

$$A_{\text{rel}} \equiv \int_0^1 \tilde{y} [1 - B_{\text{rel}}(\tilde{y})] d\tilde{y} = \text{const}. \quad (\text{A8})$$

From our numerical solutions with very high (of order 10^3) values of u_{in} , we find $A_{\text{rel}} \simeq 0.027$ and $C = -1$. Thus, we get

$$Y(u_{\text{in}} \rightarrow \infty) \simeq \frac{37}{u_{\text{in}}} \left(1 - \frac{18.5 \ln u_{\text{in}}}{u_{\text{in}}} + \dots \right). \quad (\text{A9})$$

Notice that, because of the rather large (18.5) numerical coefficient multiplying the logarithmic factor, this logarithmic correction does not become negligible until one considers really very large values of u_{in} , of order 10^3 or more. This is the reason why the plot on Figure 2 (with u_{in} up to 200) does not show a very good agreement with the simple power law $Y \sim 1/u_{\text{in}}$. Notice however, that the numerical results for values of u_{in} in the range between 200 and 2000 are in excellent agreement with the predicted asymptotic behavior (A7), as demonstrated separately in Figure 4.

Now let us consider the non-relativistic regime, $u_{\text{in}} \ll 1$. In this limit, the expression (A4) for the integral entering the first term on the rhs of equation (A3) tends to 1 (this is of course a trivial result since in this limit $\gamma(\tilde{y}) \approx 1$). Then, since $\beta_{\text{in}} \approx u_{\text{in}}$ in this regime, this first term can be evaluated simply as u_{in} .

At the same time, just as in the strongly relativistic case, the function $\hat{B}(\tilde{y})$ also approaches a certain universal profile, as can be seen in Figure 3 (we shall call this profile $\hat{B}_{\text{nr}}(\tilde{y})$). Then, the integral entering the second term on the rhs of equation (A3) asymptotically approaches a constant value

$$\int_0^1 \tilde{y} B(\tilde{y}) d\tilde{y} \rightarrow \frac{1}{2} - A_{\text{nr}} = \text{const}, \quad (\text{A10})$$

where we defined A_{nr} in a manner similar to A_{rel} :

$$A_{\text{nr}} \equiv \int_0^1 \tilde{y} [1 - B_{\text{nr}}(\tilde{y})] d\tilde{y}. \quad (\text{A11})$$

Thus, we see that in the non-relativistic limit the function $Y(u_{\text{in}})$ asymptotically approaches an inverse power law:

$$Y(u_{\text{in}}) \simeq \frac{1}{u_{\text{in}}} \frac{1}{\frac{1}{2} + A_{\text{nr}}} \simeq \frac{1.71}{u_{\text{in}}}, \quad (\text{A12})$$

where we used the value of $A_{\text{nr}} = 0.0855$ computed using our numerical solution for the case $u_{\text{in}} = 0.01$. The resulting asymptotic behavior in the non-relativistic regime agrees very well with the numerical results, as can be seen in Figure 2.

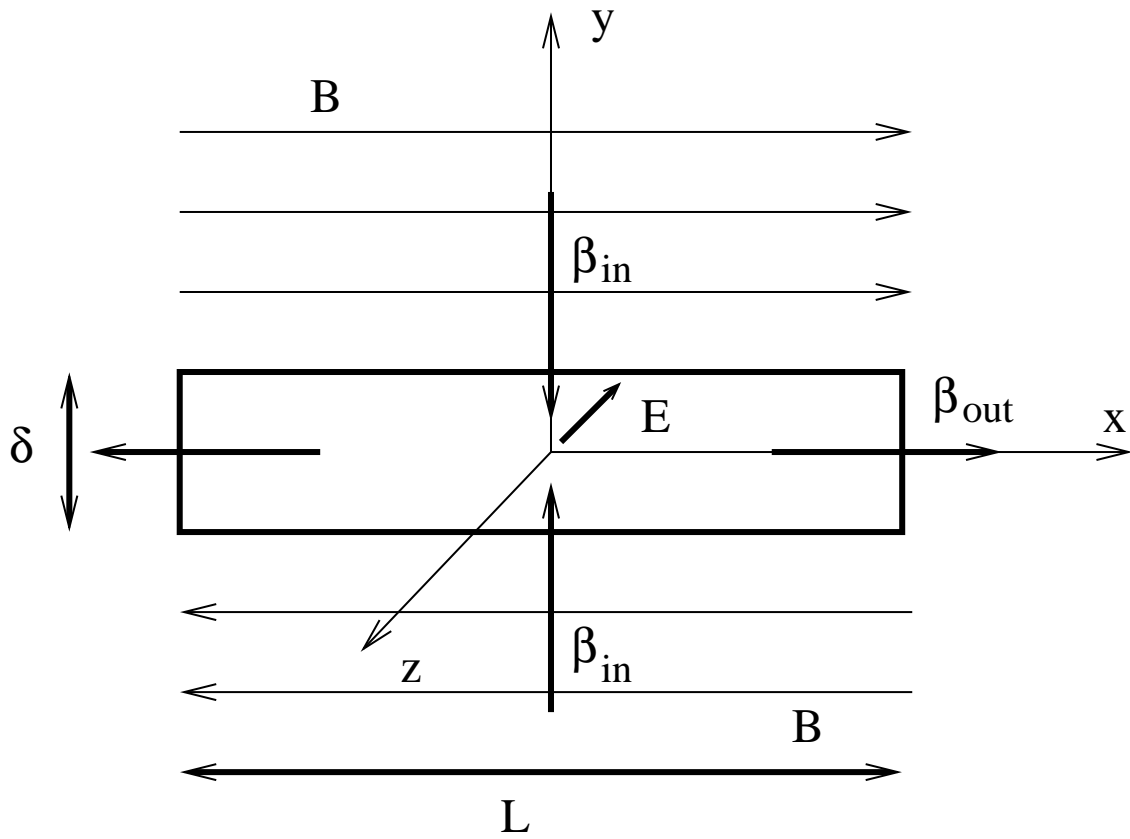


Fig. 1.— Geometry of the model. The reconnection layer has a width L in x direction and thickness δ in y direction (and infinite depth in z). Outside there is strongly magnetized plasma flowing into the reconnection layer with velocity β_{in} along the y direction. Inside

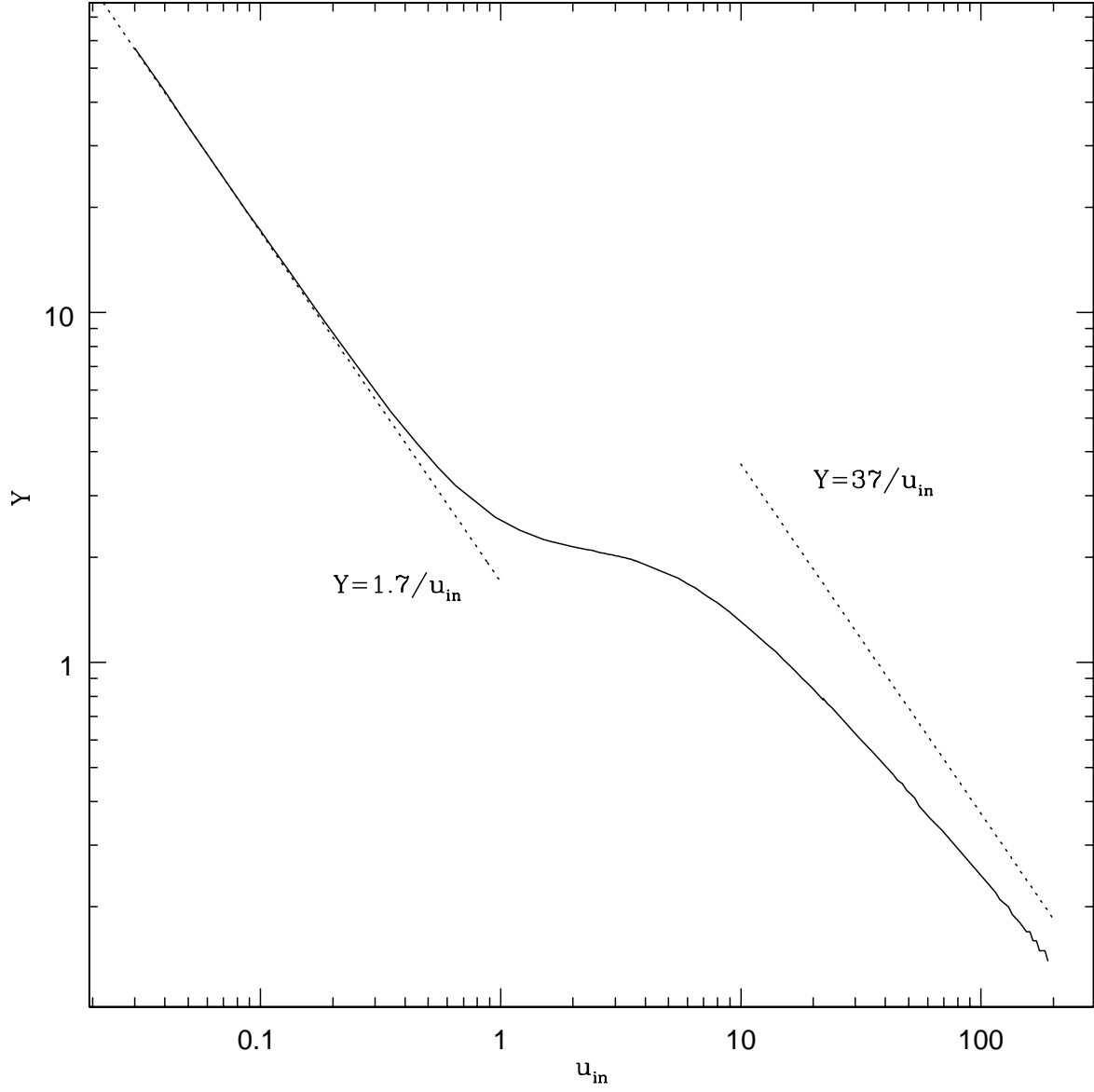


Fig. 2.— Dependence of $Y \equiv \delta/\eta$ on the four velocity of the incoming plasma for a linear dependence of $u(y) = u_{\text{in}}y/\delta$ inside the reconnection layer. The non-relativistic asymptotic is $Y = 1.7/u_{\text{in}}$.

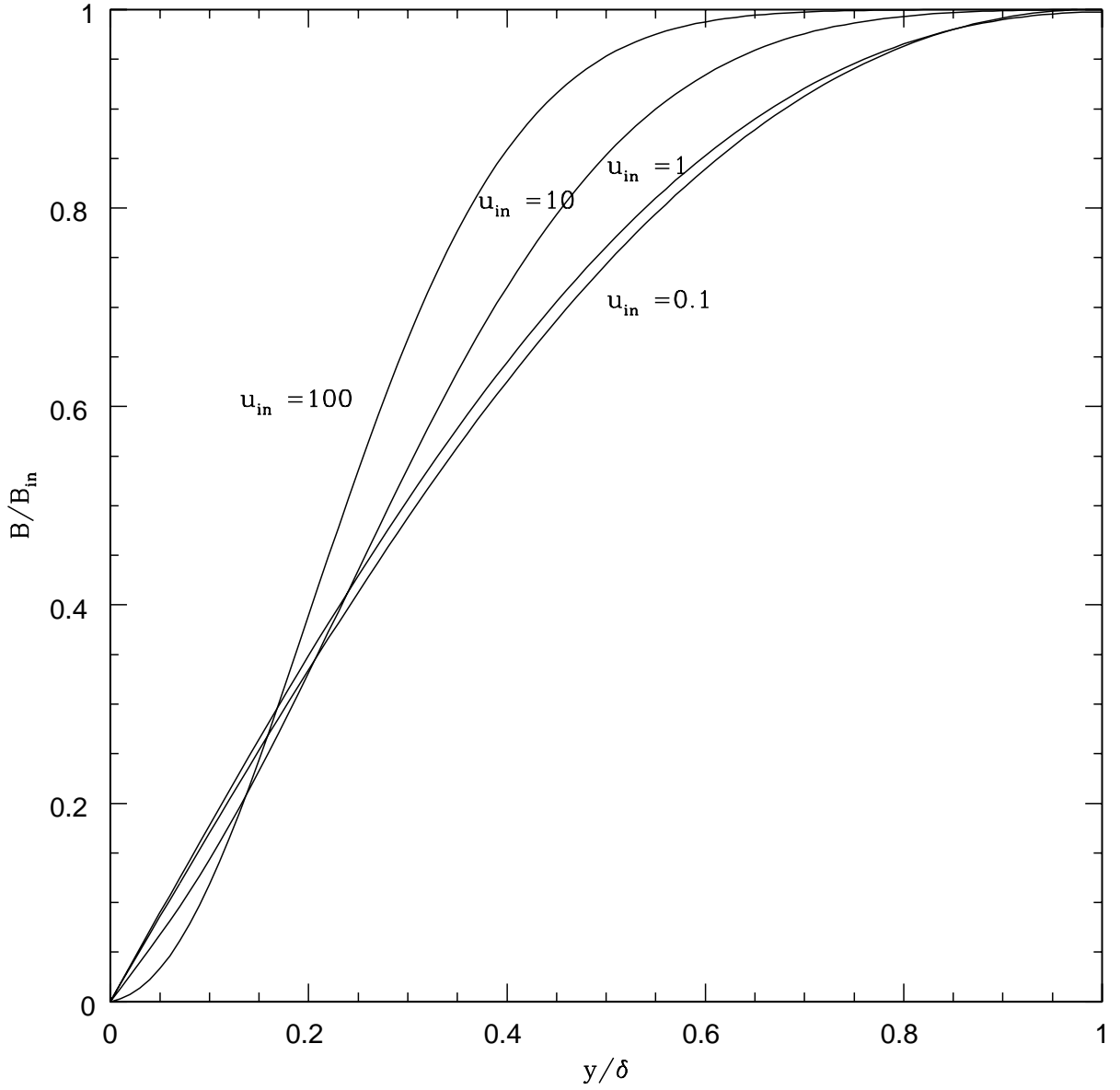


Fig. 3.— Structure of the magnetic field for a linear dependence of $u(y) = u_{in}y/\delta$ for different values of u_{in} .

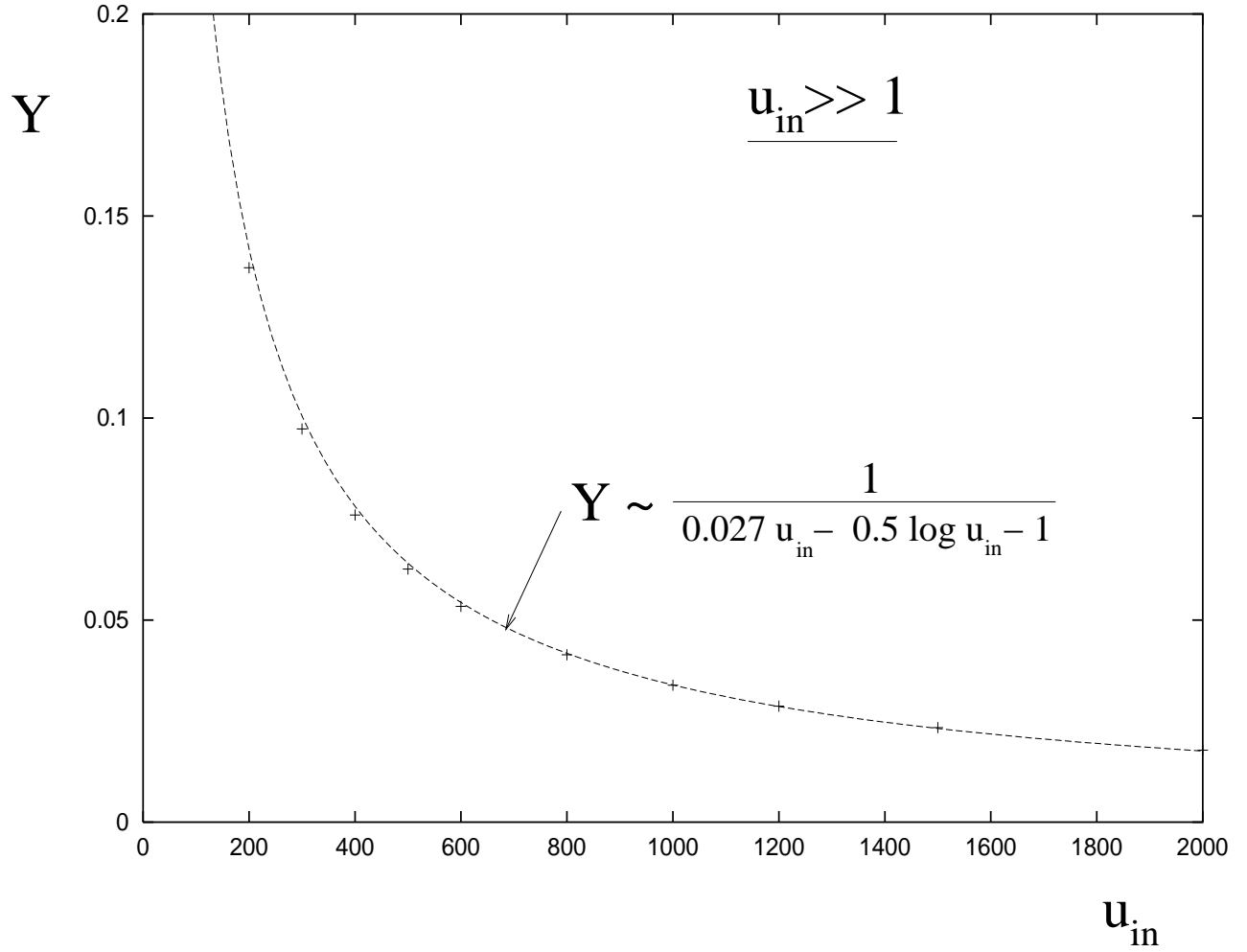


Fig. 4.— Asymptotic behavior of the function $Y(u_{\text{in}})$ in the strongly-relativistic limit $u_{\text{in}} \rightarrow \infty$.